

## Supplementary Information

### Determination of proton concentration at cardiolipin-containing membrane interface and its relation with peroxidase activity of cytochrome *c*

Partha Pratim Parui,<sup>\*a,b</sup> Yeasmin Sarakar,<sup>a</sup> Rini Majumder,<sup>a</sup> Sanju Das,<sup>a,c</sup> Hongxu Yang,<sup>b</sup> Kazuma Yasuhara,<sup>b</sup> and Shun Hirota<sup>\*b</sup>

<sup>a</sup>*Department of Chemistry, Jadavpur University, Kolkata 700032, India.*

<sup>b</sup>*Division of Materials Science, Graduate School of Science and Technology, Nara Institute of Science and Technology, Nara 630-0192, Japan.*

<sup>c</sup>*Department of Chemistry, Maulana Azad College, Kolkata 700013, India.*

#### Contents

<b>Fig. S1.</b>	Phase contrast microscopic observation of GUVs.	... p. S3
<b>Fig. S2.</b>	UV-vis absorption spectra of LUV in the presence and absence of RHG.	... p. S4
<b>Fig. S3.</b>	Fluorescence spectra of RHG in the presence of various concentrations of LUV.	... p. S5
<b>Fig. S4.</b>	RHG- and LUV-concentration dependences of its fluorescence intensity in the presence of DOPC/DOPE/TOCL LUV.	... p. S6
<b>Fig. S5.</b>	LUV-concentration dependence of UV-vis absorption and fluorescence spectra of RHG.	... p. S7
<b>Fig. S6.</b>	Fluorescence quantum yield of RHG in the presence of DOPC/DOPE/TOCL LUV.	... p. S8
<b>Fig. S7.</b>	Optical absorbance of RHG at 535 nm in the presence of various concentrations of DOPG/DOPE/CL LUV.	... p. S9
<b>Fig. S8.</b>	UV-vis absorption spectra (at pH 2.0) of the solution obtained after filtration of the RHG solution containing DOPC/DOPE/TOCL LUV at pH 4.5–8.0.	... p. S10
<b>Fig. S9.</b>	RHG fluorescence quenching studies by an addition of Cu(ClO <sub>4</sub> ) <sub>2</sub> /Na <sub>2</sub> S in the presence of DOPC/DOPE/TOCL LUV.	... p. S11
<b>Fig. S10.</b>	UV-vis absorption and fluorescence spectra of RHG in the presence of DOPG, DOPC, or DOPE LUV.	... p. S12

<b>Fig. S11.</b>	pH-dependence of UV-vis absorption and fluorescence spectra of RHG in the presence and absence of LUV.	... p. S13
<b>Fig. S12.</b>	pH-dependences of UV-vis absorption and fluorescence spectra of RHG in buffer containing ethanol.	... p. S14
<b>Fig. S13.</b>	UV-vis absorption spectra of PMP in the presence of LUV. ... p. S15	
<b>Fig. S14.</b>	UV-vis absorption spectra of mitoplast.	... p. S16
<b>Fig. S15.</b>	Plots of $X_{o-RHG}$ ( $[o-RHG]/[RHG]$ ) against bulk pH in the presence and absence of LUV formed with the lipids extracted from the mitochondrial membrane and in the absence of LUV.	... p. S17
<b>Fig. S16.</b>	Plots of $X_{o-RHG}$ ( $[o-RHG]/[RHG]$ ) against bulk pH in the presence of DOPC/TOCL and DOPC/DOPE/TOCL LUVs and in the absence of LUV.	... p. S18
<b>Fig. S17.</b>	Fluorescence spectra of RHG in presence of DOPC/DOPE/TOCL LUV containing different TOCL%.	... p. S19
<b>Fig. S18.</b>	Interface pH' ( $-\log[H^+]$ ) plotted against TOCL% in DOPC/DOPE/TOCL LUV.	... p. S20
<b>Fig. S19.</b>	UV-vis absorption and fluorescence spectra of RHG in the presence of DOPC/DOPG LUV.	... p. S21
<b>Fig. S20.</b>	Fluorescence spectra of RHG in the presence of DOPC/DOPE/TOCL LUV and cyt <i>c</i> .	... p. S22
<b>Fig. S21.</b>	Fluorescence spectra of RHG in the presence and absence of cyt <i>c</i> .	... p. S23
<b>Fig. S22.</b>	DSC thermograms of oxidized cyt <i>c</i> at various pH.	... p. S24
<b>Fig. S23.</b>	UV-vis absorption spectra of oxidized cyt <i>c</i> before and after incubation at 85°C.	... p. S25
<b>Fig. S24.</b>	UV-vis absorption spectra of oxidized cyt <i>c</i> in the presence of H <sub>2</sub> O <sub>2</sub> and 2-methoxyphenol with and without DOPC/DOPE/TOCL LUV.	... p. S26
<b>Fig. S25.</b>	TOCL concentration dependence on the cyt <i>c</i> -catalysed ABTS oxidation rate with DOPC/DOPE/TOCL LUV.	... p. S27
<b>Fig. S26.</b>	Plots of $X_{o-RHG}$ ( $[o-RHG]/[RHG]$ ) against bulk pH in the presence of DOPC/DOPE/CL LUV containing different ratio of CL (TOCL and TMCL).	... p. S28
<b>Fig. S27.</b>	NMR spectrum of RHG.	... p. S29

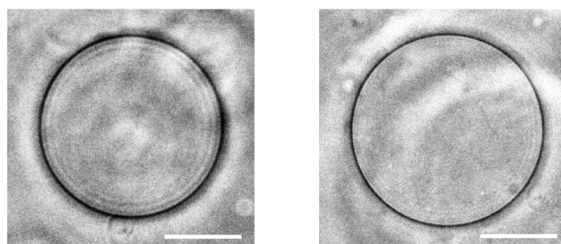


**Fig. S1.** Phase contrast microscopic observation of (a) DOPC/DOPE/TOCL (2:1:1) and (b) DOPG/DOPC (2:1) GUVs in 1 mM HEPES buffer, pH 6.5, containing 200 mM sucrose at 25°C. RHG was added to the solution for 0.06% of the total lipid amount. White bars represent 5  $\mu$ m.

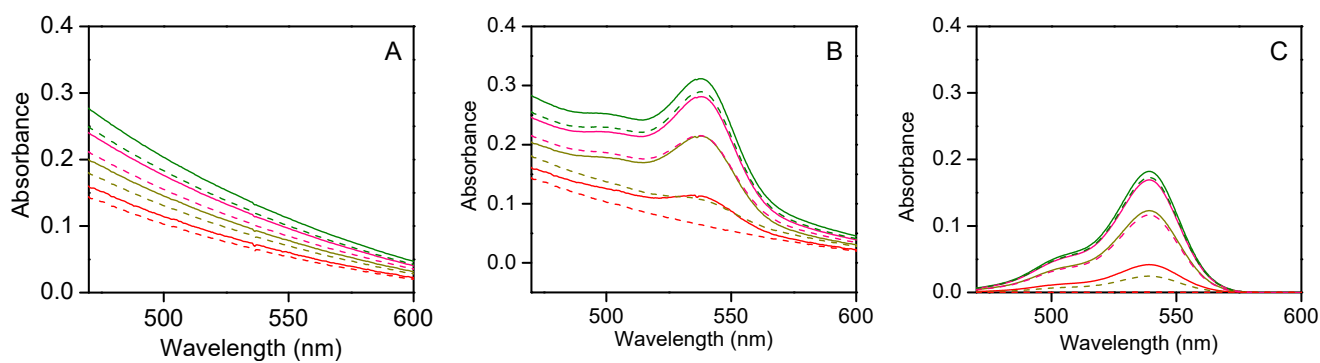


**Fig. S2.** UV-vis absorption spectra of DOPC/DOPE/TOCL (2:1:1) (solid lines) and DOPG (broken lines) LUVs (total lipid, 2 mM) in (A) the absence and (B) presence of RHG (2  $\mu$ M), and (C) their difference spectra at various pH: green, 4.0; pink, 5.0; dark yellow, 6.0; red, 7.0.

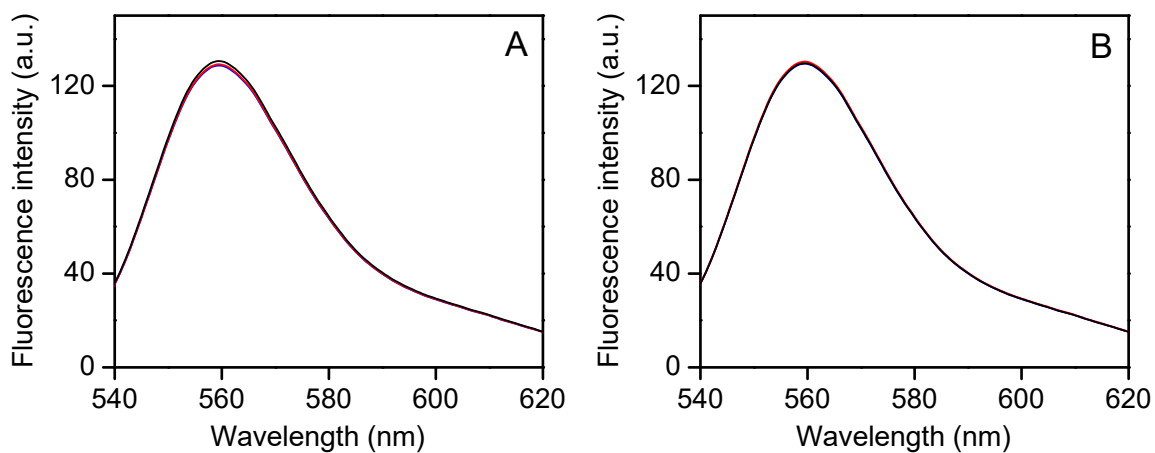


**Fig. S3.** Fluorescence spectra of RHG (0.2  $\mu$ M) in the presence of various concentrations of (A) DOPC/DOPE/TOCL (2:1:1) LUV at pH 4.5 and (B) DOPG LUV at pH 4.0. Total lipid concentration: black, 0.2 mM; blue, 0.5 mM and red, 1 mM.

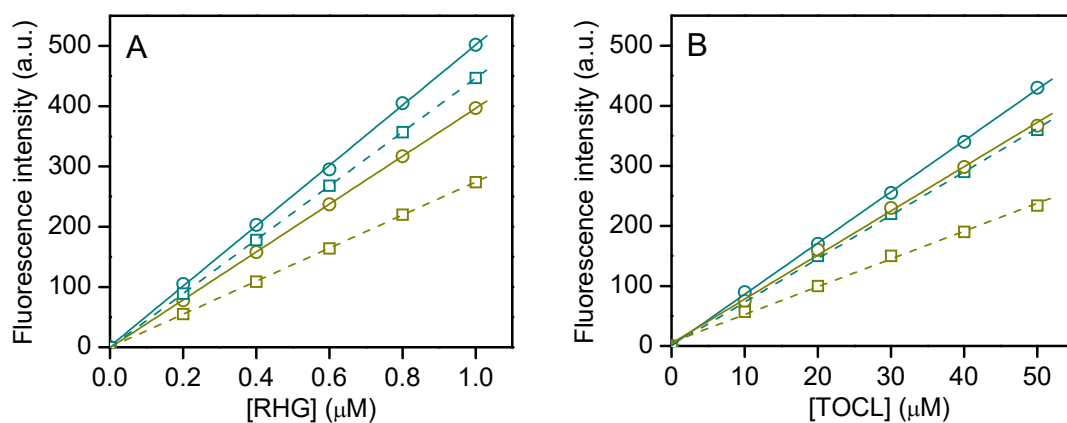


**Fig. S4.** (A) RHG concentration dependence of its fluorescence intensity in the presence of DOPC/DOPE/TOCL LUV ([RHG]:[total lipid]=1:1000; DOPC:DOPE=2:1; TOCL, 10% (square, broken line) and 25% (circle, solid line)). (B) TOCL concentration dependence of RHG (1  $\mu\text{M}$ ) fluorescence intensity in the presence of DOPC/DOPE/TOCL LUV (DOPC:DOPE=2:1; TOCL, 10% (square, broken line) and 25% (circle, solid line)). The fluorescence intensity was measured at 560 nm at various pH: dark cyan, pH 5.5; dark yellow, 6.0.

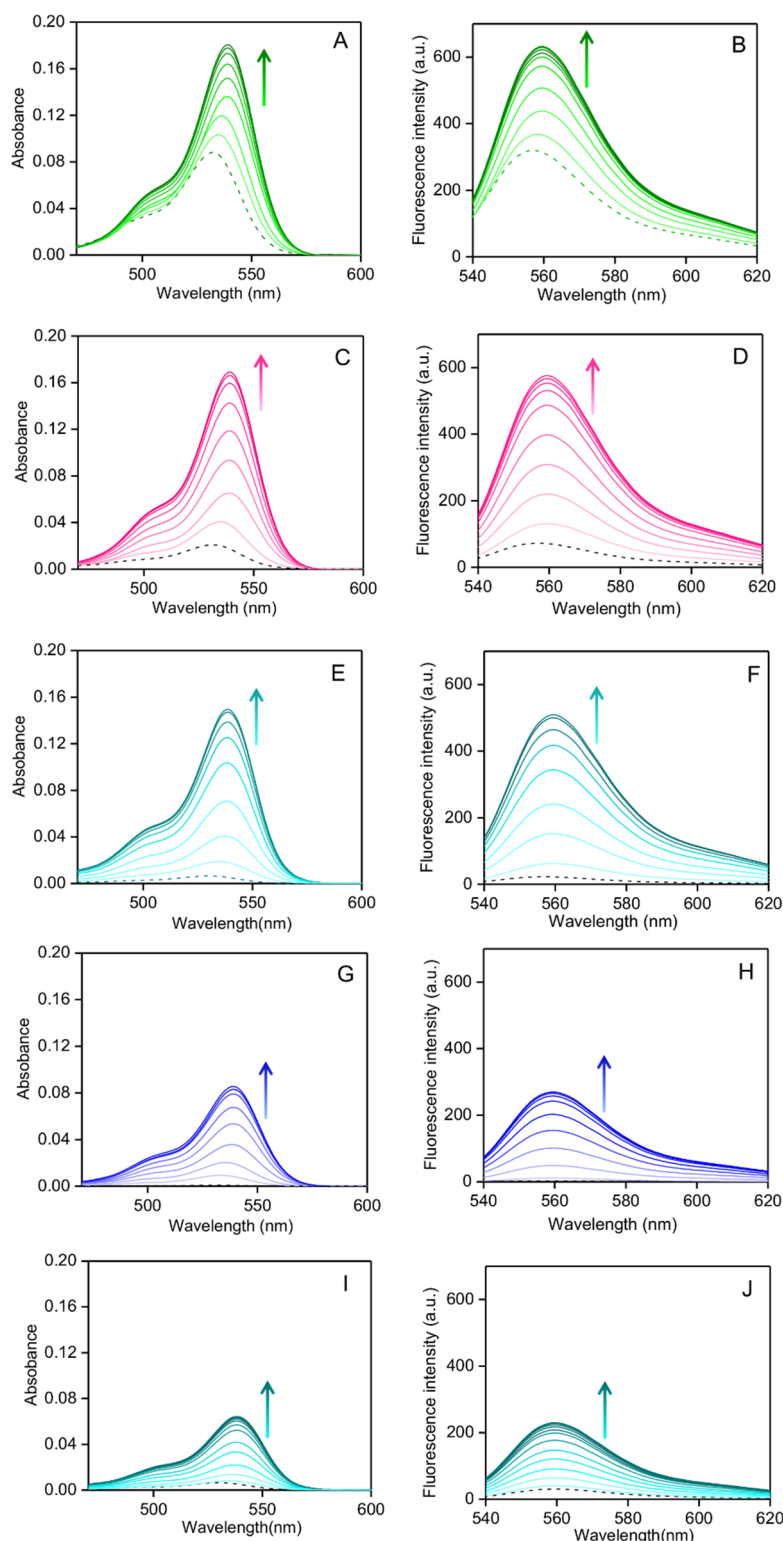


**Fig. S5.** LUV-concentration dependence of (A,C,E,G,I) UV-vis absorption and (B,D,F,H,J) fluorescence spectra of RHG in the presence of LUV: (A–H) DOPC/DOPE/TOCL (2:1:1) and (I,J) DOPG LUVs. The spectra were measured at 25°C at various pH: (A,B) 4.0, (C,D) 5.0, (E,F,I,J) 5.5, and (G,H) 6.5. RHG concentrations for the absorption and fluorescence measurements were 2 and 1  $\mu\text{M}$ , respectively. The total lipid concentrations of LUV were 0.06, 0.12, 0.20, 0.32, 0.40, 0.50, 0.60, 1.50, and 2.00 mM for absorption measurements and 0.03, 0.06, 0.10, 0.16, 0.20, 0.25, 0.30, 0.75, and 1.00 mM for fluorescence measurements. The spectra of RHG in the absence of LUV are depicted in broken lines for comparison. The increases in intensities by increasing the LUV concentrations are indicated in arrows.

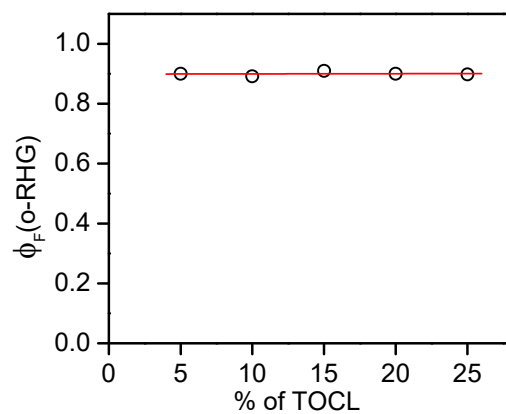


**Fig. S6.** Fluorescence quantum yield of RHG in the presence of DOPC/DOPE/TOCL LUV with various TOCL%. Experimental conditions: RHG, 1.0  $\mu\text{M}$ ; total lipid concentration, 1.0 mM; DOPC:DOPE=2:1; TOCL, 5–25%; pH, 3.0; temperature, 25°C.

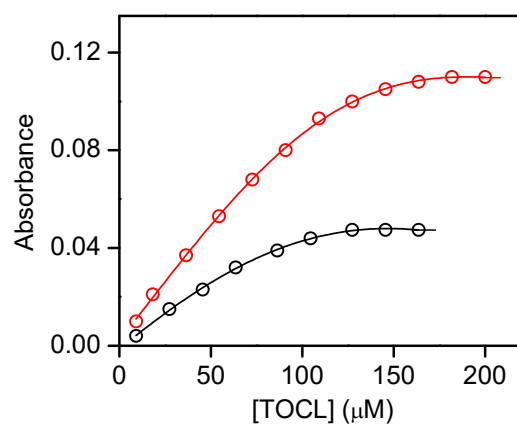


**Fig. S7.** Optical absorbance of RHG (2  $\mu\text{M}$ ) at 535 nm in 10 mM HEPES buffer, pH 6.2, in the presence of various concentrations of TOCL obtained by changing the DOPG/DOPE/TOCL LUV (DOPC:DOPE=2:1; CL, 10 (black) and 25% (red) of total lipids) concentration.

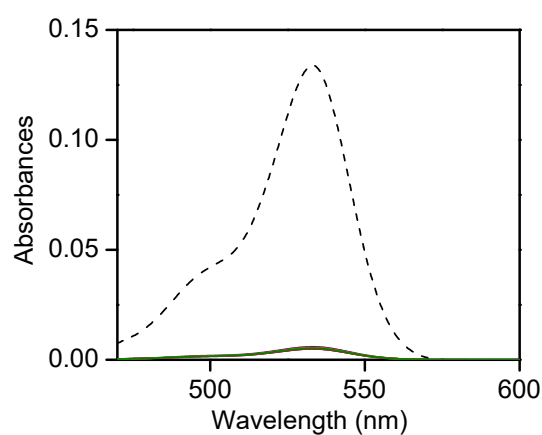


**Fig. S8.** UV-vis absorption spectra of the solution obtained after filtration of the RHG (2.0  $\mu\text{M}$ ) solution containing DOPC/DOPE/TOCL (2:1:1) LUV (total lipid, 2.0 mM) at pH 4.5–8.0 (solid lines) and that of RHG (2.0  $\mu\text{M}$ ) not containing LUV (broken black line). The RHG solutions in the presence of LUV were prepared at various pH: purple, 4.5; dark yellow, 5.8; blue, 6.3; red, 6.8; orange, 7.3 and green, 8.0. Filtration was performed with a 100K molecular weight cut-off filter. The spectra of the filtrates were monitored after adjusting their pH to 2.0. The spectra were measured at pH 2.0 and 25°C.

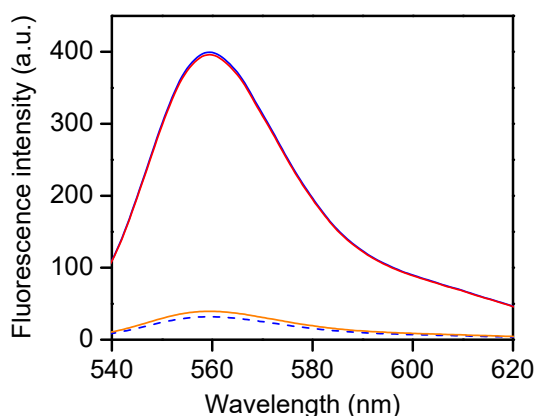


**Fig. S9.** Fluorescence spectra of RHG (1  $\mu$ M) in the presence of DOPC/DOPE/TOCL (2:1:1) LUV before and after an addition of  $\text{Cu}(\text{ClO}_4)_2/\text{Na}_2\text{S}$ . RHG in 10 mM cacodylate buffer, pH 6.0, containing DOPC/DOPE/TOCL (2:1:1) LUV was concentrated using a cut-off filter, and subsequently diluted with 10 mM HEPES buffer, pH 8.0. The pH of the diluted solution was adjusted to pH 8.0, and the spectrum of the solution was measured (orange). Individually, the DOPC/DOPE/TOCL (2:1:1) LUV solution at pH 6.0 was concentrated, and the concentrated solution containing LUV was mixed with the filtrate. The fluorescence spectra of the mixture were measured before (solid blue) and after (broken blue) an addition of  $\text{Cu}(\text{ClO}_4)_2/\text{Na}_2\text{S}$  (1:2) (total salt, 2 mM). The spectrum of RHG (1  $\mu$ M) in 10 mM cacodylate buffer, pH 6.0, in the presence of DOPC/DOPE/TOCL (2:1:1) LUV (total lipid, 1 mM) is shown in a solid red line for comparison.

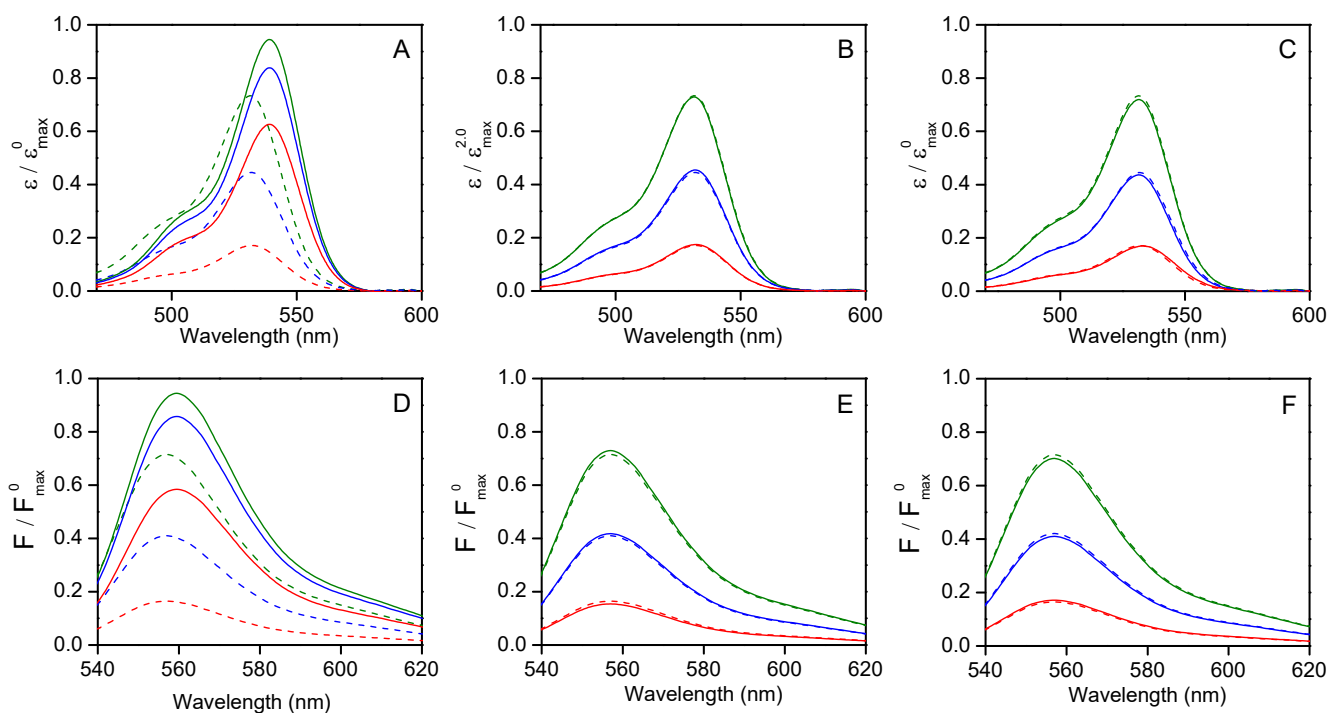


**Fig. S10.** UV-vis (A–C) absorption and fluorescence (D–F) spectra of RHG in the presence (solid lines) and absence (broken lines) of DOPG (A and D), DOPC (B and E), and DOPE (C and F) LUV at various pH: green, pH 4.0; blue, pH 4.5; red, pH 5.0. The molar extinction coefficient ( $\epsilon$ ) and fluorescence intensity ( $F$ ) are divided by the maximum  $\epsilon$  and  $F$  values of the corresponding solution at pH 2.0 ( $\epsilon_{\max}^0$  and  $F_{\max}^0$ ), respectively. RHG concentrations were 2 and 1  $\mu\text{M}$  for absorption and fluorescence experiments, respectively. LUV concentrations (total lipid) were 2.0 and 1.0 mM for absorption and fluorescence experiments, respectively.

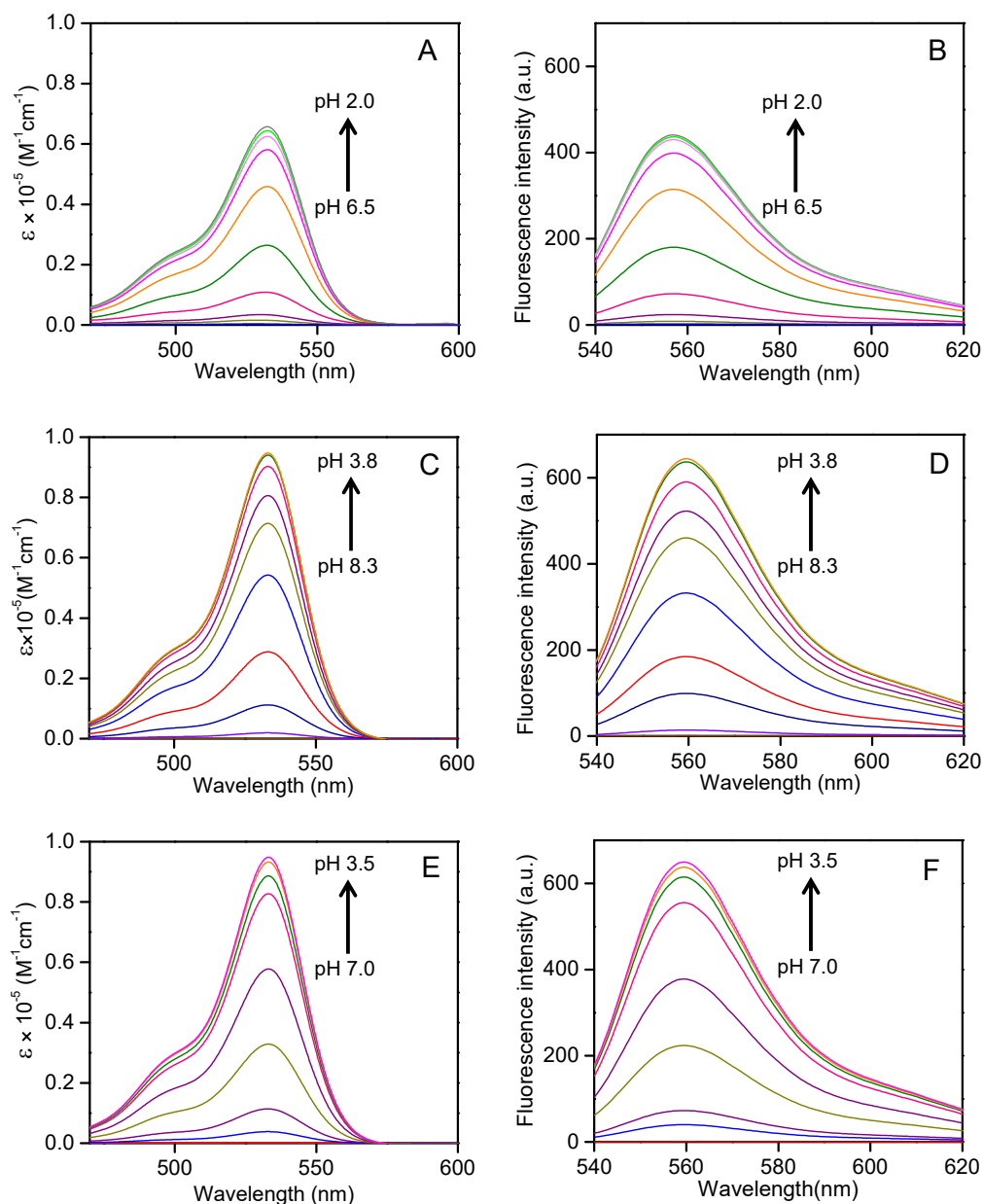


**Fig. S11.** pH-dependence of (A,C,E) UV-vis absorption and (B,D,F) fluorescence spectra of RHG in the presence and absence of intensity-saturated concentration of LUV (RHG:lipid=1:1000) at 25°C: (A,B) without LUV (pH: 6.5, 6.0, 5.5, 5.0, 4.5, 4.0, 3.5, 3.0, 2.5, and 2.0), (C,D) with DOPC/DOPE/TOCL (2:1:1) LUV (pH: 8.3, 7.8, 7.3, 6.8, 6.3, 5.8, 5.3, 4.8, 4.3, and 3.8), and (E,F) with DOPG LUV (pH: 7.0, 6.5, 6.0, 5.5, 5.0, 4.5, 4.0, and 3.5). The increases in intensities by decreasing pH are indicated in arrows. The RHG concentrations for the absorption and fluorescence measurements were 2 and 1  $\mu$ M, respectively. Buffer: pH 2.0–5.0, citrate-phosphate buffer (mixture of 10 mM sodium phosphate and 10 mM sodium citrate solutions); pH 5.0–6.0, 10 mM cacodylate buffer; pH 6.0–8.3, 10 mM HEPES buffer.

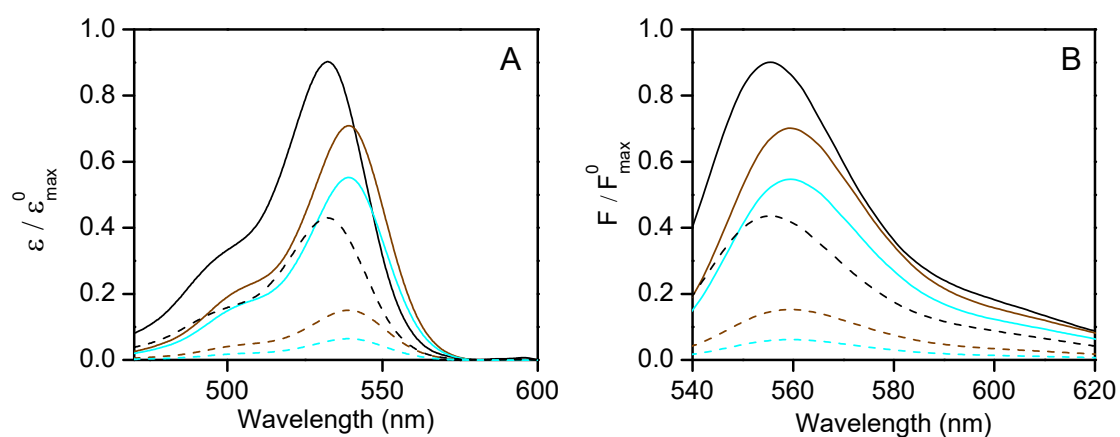


**Fig. S12.** pH-dependences of (A) UV-vis absorption and (B) fluorescence spectra of RHG in citrate-phosphate buffer (mixture of 10 mM sodium phosphate and 10 mM sodium citrate solutions), containing 35% (brown) and 58% (w/w) (cyan) ethanol at pH 3.5 (solid line) and 4.5 (broken line) at 25°C. The spectra of RHG in citrate-phosphate buffer at the corresponding pH are depicted in black. The RHG concentrations for the absorption and fluorescence measurements were 2 and 1  $\mu\text{M}$ , respectively. The molar extinction coefficient ( $\varepsilon$ ) and fluorescence intensity ( $F$ ) are divided by the maximum  $\varepsilon$  and  $F$  values of the corresponding solution at pH 1.5 ( $\varepsilon_{\text{max}}^0$  and  $F_{\text{max}}^0$ ), respectively.

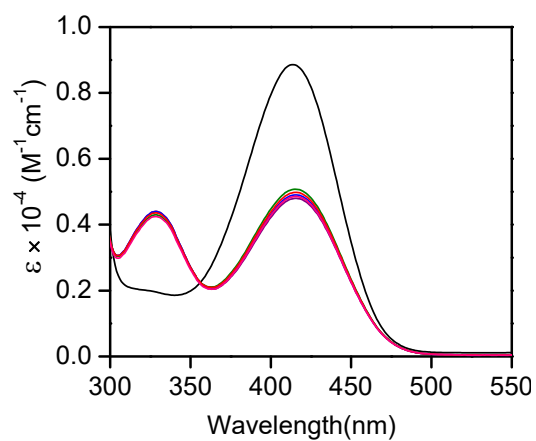


**Fig. S13.** UV-vis absorption spectra of PMP (2.0  $\mu\text{M}$ ) in the presence of intensity-saturated concentrations of LUV (total lipid, 3 mM) in 10 mM HEPES buffer, pH 6.5, at 25°C: pink, lipids from mitochondrial membrane; red, DOPC/DOPE/TOCL (2:1:1); green, DOPC/DOPE (2:1); purple, DOPG; blue, DOPC. The spectrum of PMP (2.0  $\mu\text{M}$ ) in the absence of LUV is depicted in black for comparison.

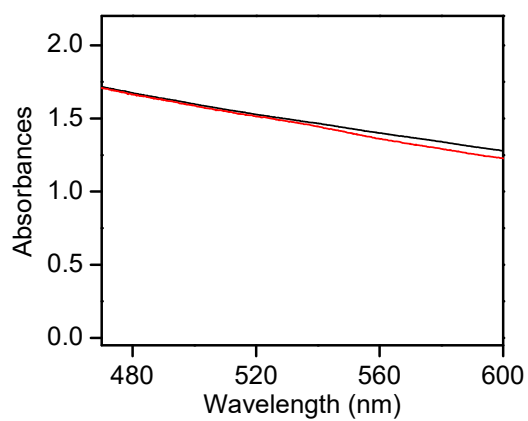


**Fig. S14.** UV-vis absorption spectra of mitoplast (total lipid, ~0.1 mM) in the presence (red) and absence (black) of RHG (1  $\mu$ M) in 10 mM HEPES buffer, pH 6.8.

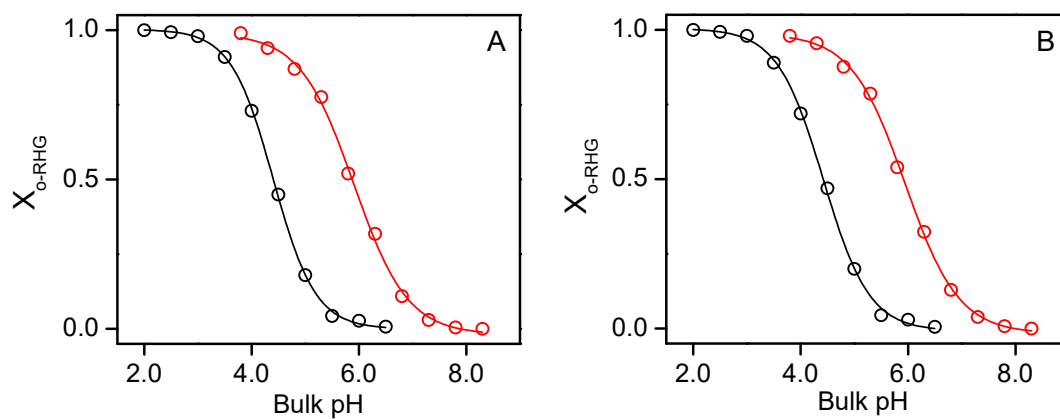


**Fig. S15.** Plots of  $X_{o-RHG}$  ( $[o-RHG]/([RHG])$ ) against bulk pH in the presence (red) of LUV formed with the lipids extracted from the mitochondrial membrane measured under LUV-binding saturation conditions and in the absence of LUV (black): analysed with (A) absorption and (B) fluorescence spectra. Measurements were performed at 25°C.

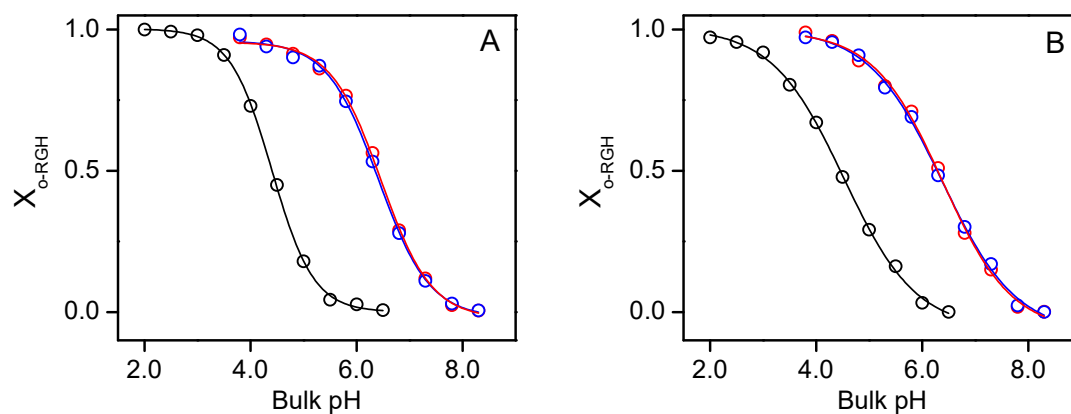


**Fig. S16.** Plots of  $X_{o-RHG}$  ( $[o-RHG]/([RHG])$ ) against bulk pH in the presence of DOPC/TOCL (3:1) (blue) and DOPC/DOPE/TOCL (2:1:1) (red) LUVs measured under TOCL-binding saturation conditions and in the absence of LUV (black) at 25°C: analysed with (A) absorption and (B) fluorescence spectra.

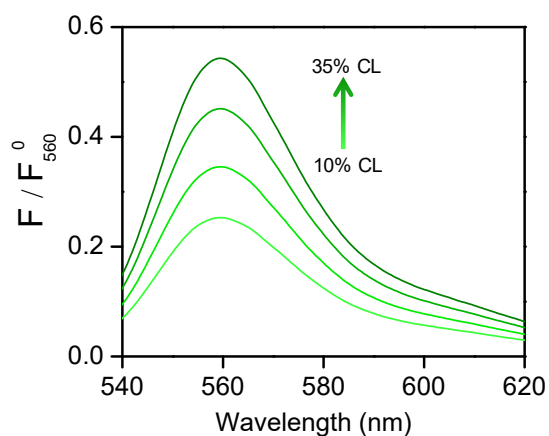


**Fig. S17.** Fluorescence intensity of RHG (1  $\mu$ M) in the presence of DOPC/DOPE/TOCL LUV containing different TOCL% (DOPC:DOPE=2:1; TOCL, 10, 15, 25, and 35%; total lipid, 1 mM) in 10 mM HEPES buffer, pH 6.5, 25°C. The fluorescence intensity (F) is divided by the F value at 560 nm of the corresponding solution at pH 3.0 ( $F_{560}^0$ ). The fluorescence intensity was saturated (against LUV concentration) for all LUV concentrations used.

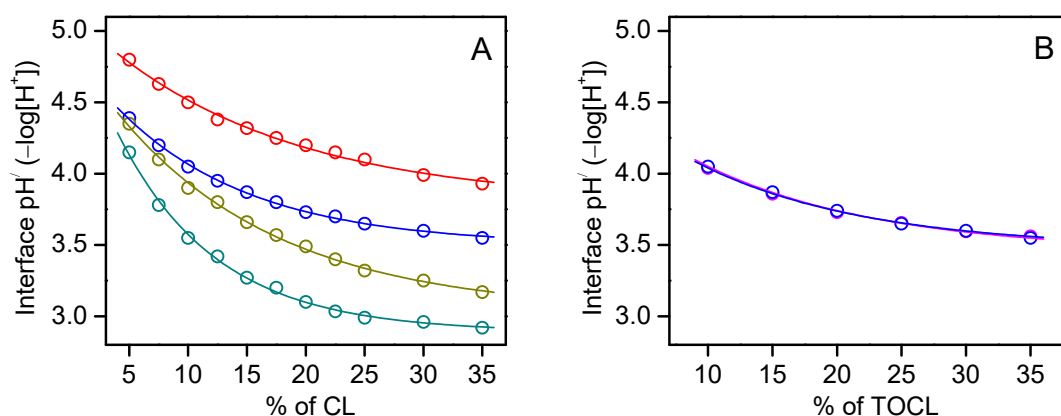


**Fig. S18.** (A) Interface pH' ( $-\log[H^+]$ ) plotted against TOCL% in DOPC/DOPE/TOCL LUV (total lipid, 1.0 mM; DOPC/DOPE=2:1; TOCL=5–35%) at various bulk pH: red, 7.0; blue, 6.5; dark yellow, 6.0; dark cyan, 5.5. (B) Interface pH' plotted against TOCL% in DOPC/DOPE/CL LUV (red,  $[DOPC] = 360$ ,  $[DOPE] = 180 \mu\text{M}$ , TOCL: 60–290  $\mu\text{M}$ ; blue, constant total lipid concentration of 1 mM, DOPC/DOPE=2:1, TOCL=10–35%). Interface pH' values were estimated from fluorescence spectra of RHG measured at 25°C.

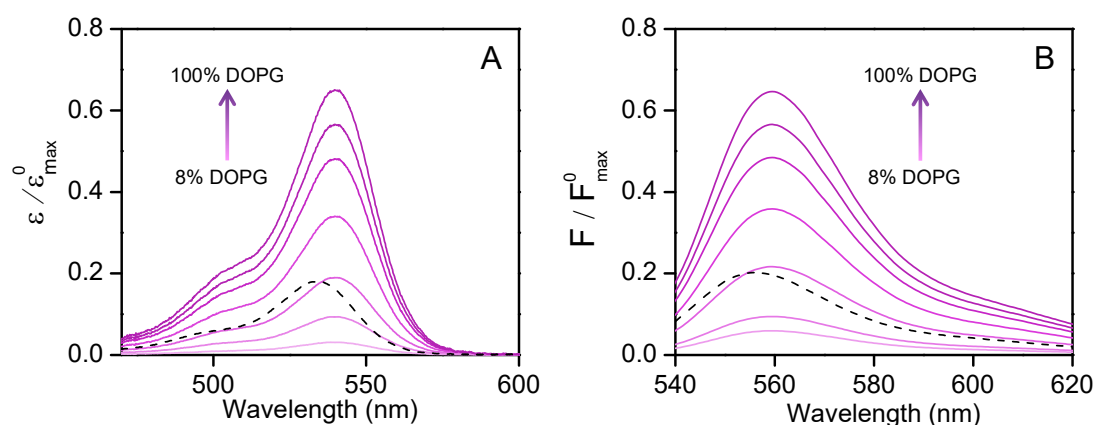


**Fig. S19.** (A) UV-vis absorption and (B) fluorescence spectra of RHG in the presence of DOPC/DOPG (DOPG: 8, 13, 27, 43, 62, 78, and 100% of total lipid) LUV in 10 mM cacodylate buffer, pH 5.0, at 25°C (purple). The spectra of RHG in the absence of LUV at pH 5.0 are shown in black broken lines. The RHG concentrations for the absorption and fluorescence measurements were 2 and 1  $\mu\text{M}$ , respectively. The molar extinction coefficient ( $\epsilon$ ) and fluorescence intensity ( $F$ ) are divided by the maximum  $\epsilon$  and  $F$  values of the corresponding solution at pH 1.5 ( $\epsilon^0_{\text{max}}$  and  $F^0_{\text{max}}$ ), respectively. The intensity changes by increasing the DOPG ratio are shown in arrows.

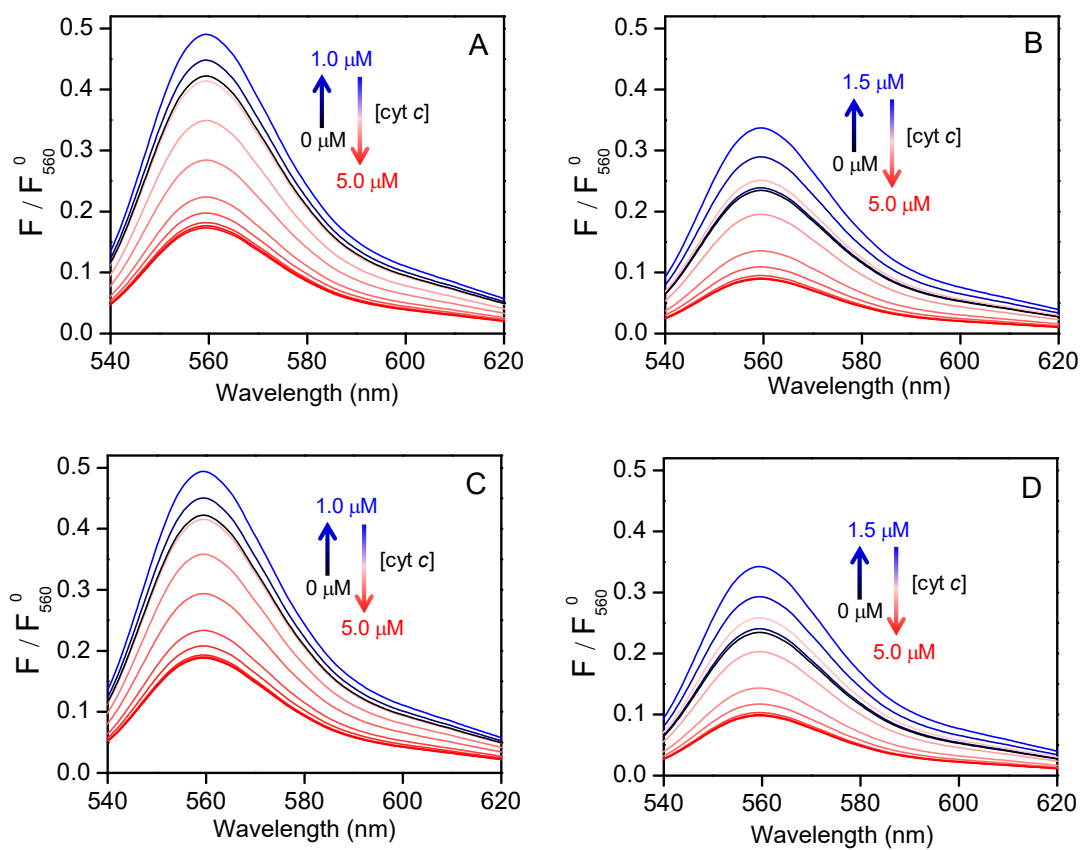


**Fig. S20.** Fluorescence spectra of RHG ( $0.05 \mu\text{M}$ ) in the presence of DOPC/DOPE/TOCL (2:1:1) LUV (total lipid,  $0.04 \text{ mM}$ ) and various concentrations of oxidized horse *cyt c* ( $0.5, 1.0, 1.5, 2.0, 2.5, 3.0, 3.5, 4.0, 4.5,$  and  $5.0 \mu\text{M}$ ) at (A) pH 6.5 and (B) 7.0. The calibrated spectra taking into account the *cyt c*-induced fluorescence intensity quenching for the spectra at pH 6.5 and 7.0 are depicted in C and D, respectively. The fluorescence intensity ( $F$ ) is divided by the  $F$  value at 560 nm of the corresponding solution at pH 3.0 ( $F_{560}^0$ ). The LUV solution after the addition of *cyt c* was incubated for 30 min. The spectra in the absence of *cyt c* are represented in black.

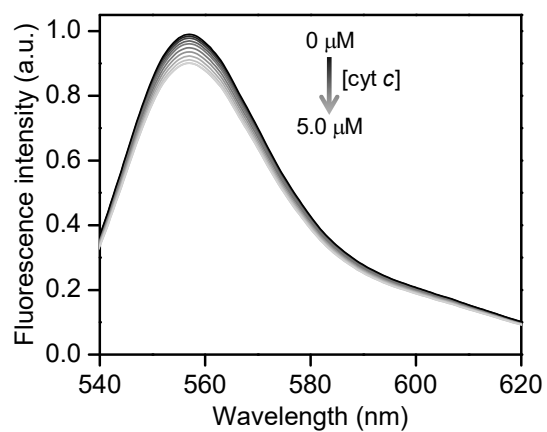


**Fig. S21.** Fluorescence spectra of RHG (0.05  $\mu\text{M}$ ) in the presence of various concentrations of oxidized horse cyt *c* (0.5, 1.0, 1.5, 2.0, 2.5, 3.0, 3.5, 4.0, 4.5, and 5.0  $\mu\text{M}$ ) and absence of it at pH 4.0.

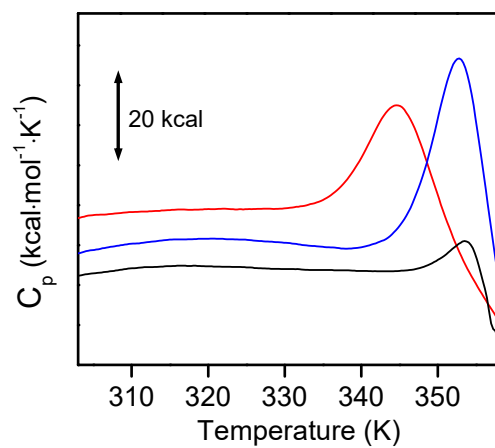


**Fig. S22.** Differential scanning calorimetry (DSC) thermograms of oxidized horse cyt *c* (100  $\mu\text{M}$ ) at various pH: red, pH 3.9; blue, pH 5.3; black, pH 6.8.

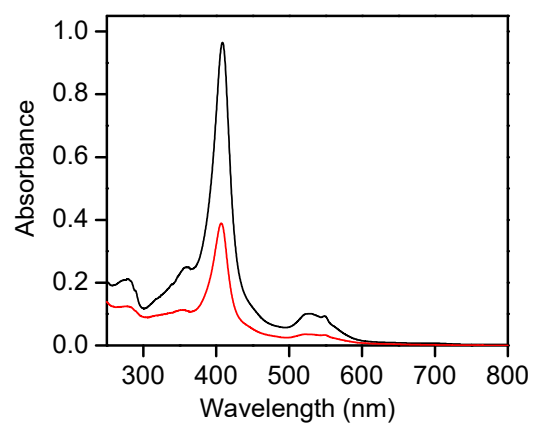


**Fig. S23.** UV-vis absorption spectra of oxidized horse cyt *c* (10  $\mu$ M) in 10 mM HEPES buffer, pH 6.8, before (black) and after (red) incubation at 85°C for 15 min. The precipitate generated by the incubation was removed with a 0.45-mm filter before the measurement.

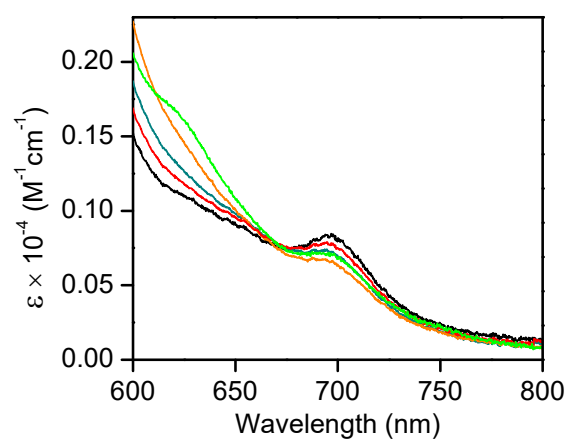


**Fig. S24.** UV-vis absorption spectra of oxidized horse cyt *c* (20  $\mu\text{M}$ ) in the presence of  $\text{H}_2\text{O}_2$  (10 mM) and 2-methoxyphenol (5  $\mu\text{M}$ ) at 25°C at various pH: orange, 3.9; dark cyan, 5.3; red, 6.8. The spectra of cyt *c* (10  $\mu\text{M}$ ) in the absence of  $\text{H}_2\text{O}_2$  and 2-methoxyphenol with (light green) and without (black) DOPC/DOPE/TOCL (2:1:1) LUV (total lipid, 500  $\mu\text{M}$ ) in 10 mM HEPES buffer, pH 6.8, are depicted for comparison. A reduced concentration of cyt *c* (10  $\mu\text{M}$ ) was used to avoid precipitation in the presence of LUV.

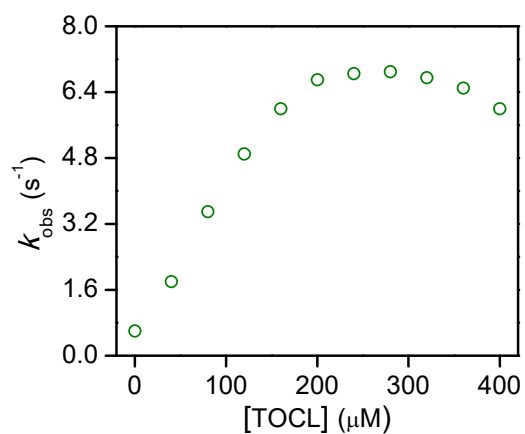


**Fig. S25.** TOCL concentration dependence of the *cyt c*-catalysed ABTS oxidation rate in the presence various concentrations of DOPC/DOPE/TOCL LUV (DOPC:DOPE=2:1; TOCL, 50% of total lipids) in 10 mM HEPES buffer, pH 6.8. Experimental conditions: *cyt c* concentration, 5 μM; DOPC/DOPE/TOCL LUV concentration, 0–800 μM (total lipid); H<sub>2</sub>O<sub>2</sub> concentration, 4 mM; ABTS, 40 μM; 25 °C.

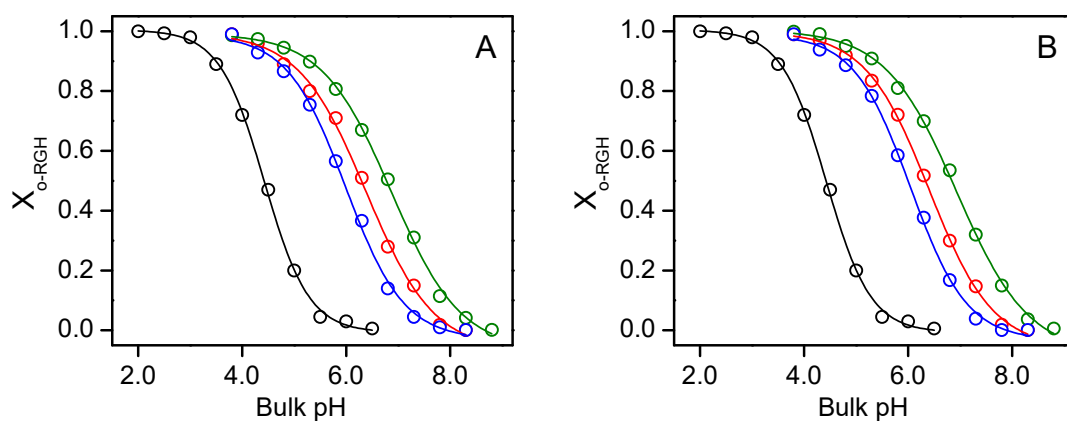


**Fig. S26.** Plots of  $X_{o\text{-RHG}}$  ( $[\text{o-RHG}]/[\text{RHG}]$ ) against bulk pH in the presence of (A) DOPC/DOPE/TOCL LUV (DOPC:DOPE=2:1, TOCL=10% (blue), 25% (red) and 50% (green) of total lipids) and (B) DOPC/DOPE/TMCL LUV (DOPC:DOPE=2:1, TMCL=10% (blue), 25% (red) and 50% (green) of total lipids) at 25°C. Similar plots in the absence of LUV (black) are shown for comparison. Fluorescence intensity saturated conditions with high LUV concentrations (lipid concentration, 1 mM) were used.

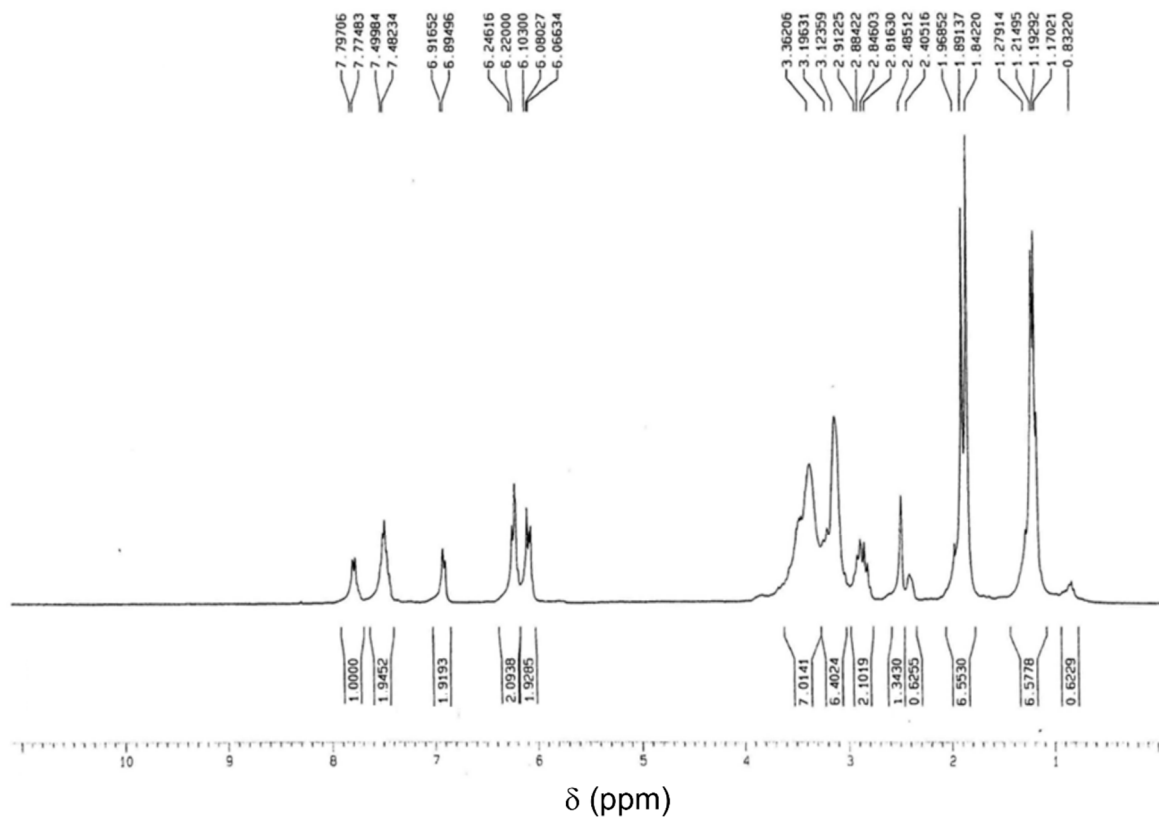


**Fig. S27.** NMR spectrum of RHG in DMSO-*d*<sub>6</sub> measured with a 300-MHz NMR spectrophotometer.